Synthesis of a series of 4-pyridyl-1,2,4-triazole-containing cadmium(II) luminescent complexes†

Bin Ding,[a] Long Yi,[a] Ying Wang,[a] Peng Cheng,*[a] Dai-Zheng Liao,[a] Shi-Ping Yan,[a] Zong-Hui Jiang,[a] Hai-Bin Song[b] and Hong-Gen Wang[b]

Received 14th June 2005, Accepted 16th September 2005
First published as an Advance Article on the web 14th November 2005
DOI: 10.1039/b508332j

Using two 4-substitued triazole ligands, 4-(pyrid-2-yl)-1,2,4-triazole (L_1) and 4-(pyrid-3-yl)-1,2,4-triazole (L_2), a series of novel triazole–cadmium(II) complexes varying from zero- to three-dimensional have been prepared and their crystal structures determined *via* single-crystal X-ray diffraction. $[Cd_2(\mu_2\text{-}L_1)_3(L_1)_2(NO_3)(\mu_2\text{-}NO_3)(H_2O)_2](NO_3)_2\cdot 1.75H_2O$ (**1**) is a binuclear complex containing bidendate, monodedate and free nitrate anions. When the bridging anions SCN^- and dca (dca = $N(CN)_2^-$) were added to the reaction system of **1**, one-dimensional (1D) $[Cd(L_1)_2(NCS)_2]_n$ (**2**) and two-dimensional (2D) $[Cd(L_1)_2(dca)_2]_n$ (**3**) were isolated, respectively. When L_2 instead of L_1 was used, $[Cd(L_2)_2(NCS)_2(H_2O)_2]$ (**4**) and 1D $[Cd(L_2)_2(dca)_2]_n$ (**5**) were obtained. When the ratio of Cd to L_2 was changed from 1 : 2 to 1 : 1 in the reaction system of **5**, three-dimensional (3D) $\{[Cd_3(\mu_2\text{-}L_2)_3(dca)_6]\cdot 0.75H_2O\}_n$ (**6**) with 1D microporous channels along the *a* direction was isolated. Further investigations on other Cd(II) salts and the L_2 ligand in a Cd to L_2 ratio of 1 : 1, an unexpected complex $[Cd(\mu_2\text{-}L_2)(\mu_3\text{-}SO_4)(H_2O)]_n$ (**7**) with a 3D open framework was obtained. All of the complexes exhibit strong blue fluorescence emission bands in the solid state at ambient temperature, of which the excitation and emission maxima are red-shifted to longer wavelength as compared to those in water. Powder X-ray diffraction and thermal studies were used to investigate the bulk nature of the 3D coordination polymers **6** and **7**.

Introduction

The study of metal coordination polymers has gained great recognition as an important interface between synthetic chemistry and materials science, and provides a solid foundation for understanding how molecules can be organized and how functionality can be achieved. Although a variety of metal coordination frameworks with beautiful topologies and interesting electronic, magnetic, and optical properties have been synthesized over the last ten years,[1–11] rational control in the construction of polymeric networks remains a great challenge in crystal engineering. The current topical areas focus on the construction of coordination polymers with novel topology and interesting properties through metal-based coordination and on the crystal engineering of molecular architectures organized by coordination bonds and supramolecular contacts (such as hydrogen bonding, π–π interactions, *etc.*).[12–15] Thus, many spectacular polymers have been documented, such as 1D chains[16] and ladders,[17] 2D grids,[18] 3D networks, interpenetrated modes, and helical staircase networks.[19] In particular, 3D porous coordination polymers with channels of different pore diameter comprised of metal ions as nodes and bridging ligands as spacers have been synthesized and need further research because of their use or anticipated use as templates to synthesize nanofibers, one-dimensional arrays of molecules, sensors, ion exchangers, and catalysts.[20]

On the other hand, coordination polymers of one-, two-, and three-dimensional infinite frameworks involving cadmium(II) ions have been the subject of great interest in recent years owing to their ability to form bonds with different donors simultaneously, the large radius, and special physical properties of the Cd(II) ion.[21–22] For instance, Fujita and co-workers have studied the catalytic activity of $\{[Cd(bipy)_2](NO_3)_2\}_n$ in the procedure of cyanosilylation reactions (bipy = 4,4′-bipyridine).[23] Several groups have investigated the fluorescence properties and the second- and third-order nonlinear optical (NLO) properties of cadmium(II) polymers.[24,25,26a] To date, the coordination polymers of cadmium(II) have been exploited using organic ligands as well as anions, *e.g.*, Cl^-, Br^-, I^-, SCN^-, N_3^-, $SeCN^-$, SO_4^{2-} *etc.*, which are an essential part of the coordination polyhedra.[26–30] The organic ligands, as well as anions, are observed to control the structural dimensionalities and stereochemistry of the cadmium(II) center. To develop further our understanding of supramolecular self-assembly, it is challenging to continue investigations on the effect of organic ligands and anions in fabricating multidimensional cadmium(II) polymers.

The field of molecular materials has known rapid development in recent years; molecular-based compounds exhibiting interesting magnetic and luminescent properties have been described.[31–34] One of the requirements to observe such macroscopic properties is to create some interactions between the molecular units or the active sites within the crystal lattices. 1,2,4-Triazole and, in particular, its derivatives are very interesting as bridging ligands. Previously, we reported a series of 3,5-substituted triazole–cadmium coordination polymers from zero- to three-dimensional tuned *via*

---

[a] *Department of Chemistry, Nankai University, Tianjin, 300071, P. R. China*
[b] *State Key Laboratory of Elemental-Organic Chemistry, Nankai University, Tianjin, 300071, P. R. China*

† Electronic supplementary information (ESI) available: TGA plot of **6** and **7**. See DOI: 10.1039/b508332j

different triazole ligands and anions.[22] We also reported the first right-helix triazole–metal complexes,[35a] some triazole–Zn(II) complexes with blue fluorescence properties, as well as triazole–Fe(II) complexes with spin-crossover properties.[35b–f] Herein we used two new 4-substituted triazole ligands 4-(pyrid-2-yl)-1,2,4-triazole (L_1) and 4-(pyrid-3-yl)-1,2,4-triazole (L_2) to synthesize a series of novel triazole–cadmium(II) complexes, namely, $[Cd_2(\mu_2\text{-}L_1)_3(L_1)_2(NO_3)(\mu_2\text{-}NO_3)(H_2O)_2](NO_3)_2\cdot1.75H_2O$ (**1**), $[Cd(L_1)_2(NCS)_2]_n$ (**2**), $[Cd(L_1)_2(dca)_2]_n$ (**3**), $[Cd(L_2)_2(NCS)_2(H_2O)_2]$ (**4**), $[Cd(L_2)_2(dca)_2]_n$ (**5**), $\{[Cd_3(\mu_2\text{-}L_2)_3(dca)_6]\cdot0.75H_2O\}_n$ (**6**) and $[Cd(\mu_2\text{-}L_2)(\mu_3\text{-}SO_4)(H_2O)]_n$ (**7**), with a variety of zero-, one-, two-, and three-dimensional structures, which were also investigated by FT-IR, luminescence properties, TGA and PXRD.

Experimental

General

The triazole ligands L_1 and L_2 were synthesized according to the literature method.[36] All other reagents were commercially available and used without further purification. The C, H, and N microanalyses were carried out with a Perkin-Elmer 240 elemental analyzer. The FT-IR spectra were recorded from KBr pellets in the range 400–4000 cm^{-1} on a Bio-Rad FTS 135 spectrometer. The photoluminescence spectrum was measured using a MPF-4 fluorescence spectrophotometer with a xenon arc lamp as the light source. Powder X-ray diffraction measurements were recorded on a D/Max-2500 X-ray diffractometer using Cu-Kα radiation. Thermal analyses (under an oxygenated atmosphere, heating rate of 5 °C min^{-1}) were carried out in a Labsys NETZSCH TG 209 Setaram apparatus.

Preparations

Synthesis of $[Cd_2(\mu_2\text{-}L_1)_3(L_1)_2(NO_3)(\mu_2\text{-}NO_3)(H_2O)_2](NO_3)_2\cdot1.75H_2O$ (1). A mixture of $Cd(NO_3)_2\cdot6H_2O$ (69 mg, 0.20 mmol), L_1 (59 mg, 0.4 mmol), and water (10 mL) was stirred for 5 h and filtered. The filtrate was kept in a $CaCl_2$ desiccator. Suitable single crystals for X-ray diffraction study were obtained after a few days, yield 25% (based on Cd(II) salts). Anal. Calc. for $C_{35}H_{33.50}Cd_2N_{24}O_{15.75}$: C, 33.47; H, 2.66; N, 26.73%. Found: C, 33.14; H, 2.64; N, 26.52%. IR (KBr): ν = 3485.1m, 3352.3w, 3280.7w, 3111.5m, 2394.6w, 1652.3w, 1559.3m, 1519.3m, 1473.2m, 1396.9s, 1241.2m, 1198.3w, 1141.5w, 1096.3m, 1025.4m, 990.7w, 884.3w, 825.2w, 778.3s, 702.1w, 639.4m, 519.7m, 457.4w cm^{-1}.

Synthesis of $[Cd(L_1)_2(NCS)_2]_n$ (2). A mixture of $Cd(NO_3)_2\cdot6H_2O$ (69 mg, 0.20 mmol), L_1 (59 mg, 0.4 mmol), NH_4SCN (19 mg, 0.4 mmol), and water (10 mL) was stirred for 5 h and filtered. The filtrate was kept in a $CaCl_2$ desiccator. The resulting solution slowly evaporated in air for a few days gaving colorless polyhedral crystals, yield 28% (based on Cd(II) salts). Anal. Calc. for $C_{16}H_{12}CdN_{10}S_2$: C, 36.89; H, 2.32; N, 26.89%. Found: C, 36.79; H, 2.36; N, 26.81%. IR (KBr): ν = 3564.6w, 3482.5m, 3235.3w, 3158.6m, 2934.6w, 2775.5w, 2567.9w, 2459.8w, 2387.7w, 2154.6s, 2110.6s, 1753.1w, 1659.2w, 1587.3m, 1511.7s, 1402.6m, 1333.9m, 1234.3s, 1196.8m, 1148.4w, 1093.7m, 1030.2s, 975.3w, 885.8m, 777.9s, 706.5m, 663.4m, 517.5m, 458.9m cm^{-1}.

Synthesis of $[Cd(L_1)_2(dca)_2]_n$ (3). A mixture of $Cd(NO_3)_2\cdot6H_2O$ (69 mg, 0.20 mmol), L_1 (59 mg, 0.4 mmol), $NaN(CN)_2$ (36 mg, 0.4 mmol), and water (10 mL) was stirred for 5 h and filtered. The filtrate was kept in a $CaCl_2$ desiccator. Suitable single crystals for X-ray diffraction study were obtained after a few days, yield 23% (based on Cd(II) salts). Anal. Calc. for $C_{18}H_{12}CdN_{14}$: C, 40.27; H, 2.25; N, 36.53%. Found: C, 40.19; H, 2.23; N, 36.49%. IR (KBr): ν = 3446.6s, 3109.5m, 2260.2m, 2213.1w, 2151.7s, 1593.4m, 1515.7s, 1478.5m, 1441.1m, 1384.4m, 1323.8m, 1242.7s, 1090.3m, 1026.1m, 886.7w, 778.9s, 714.1w, 643.4m, 524.4m, 460.4w cm^{-1}.

Synthesis of $[Cd(L_2)_2(NCS)_2(H_2O)_2]$ (4). A mixture of $Cd(NO_3)_2\cdot6H_2O$ (69 mg, 0.20 mmol), L_2 (59 mg, 0.4 mmol), NH_4SCN (19 mg, 0.4 mmol), and water (10 mL) was stirred for 5 h and filtered. The filtrate was kept in a $CaCl_2$ desiccator. After a few days, colorless crystals suitable for X-ray diffraction were obtained, yield 34% (based on Cd(II) salts). Anal. Calc. for $C_{18}H_{16}CdN_8O_2S_2$: C, 39.10; H, 2.92; N, 20.27%. Found: C, 39.04; H, 2.81; N, 20.15%. IR (KBr): ν = 3635.3s, 3570.1m, 3506.4m, 3404.7w, 3281.9w, 3135.6w, 2969.8w, 2918.9w, 2780.5w, 2356.3w, 2067.2s, 1623.4s, 1523.6m, 1400.9s, 1244.5m, 1095.3m, 1016.5m, 791.6w, 675.7w, 617.8w, 528.7w cm^{-1}.

Synthesis of $[Cd(L_2)_2(dca)_2]_n$ (5). A mixture of $Cd(NO_3)_2\cdot6H_2O$ (69 mg, 0.20 mmol), L_2 (59 mg, 0.4 mmol), $NaN(CN)_2$ (36 mg, 0.4 mmol), and water (10 mL) was stirred for 5 h and filtered. The filtrate was kept in a $CaCl_2$ desiccator. After a few days, colorless crystals suitable for X-ray diffraction were obtained, yield 34% (based on Cd(II) salts). Anal. Calc. for $C_{36}H_{24}Cd_2N_{28}$: C, 40.27; H, 2.25; N, 36.53%. Found: C, 40.21; H, 2.23; N, 36.50%. IR (KBr): ν = 3668.2m, 3407.5m, 3203.2w, 3104.9s, 3056.5w, 2294.1s, 2225.4s, 2161.1s, 1737.1w, 1578.7m, 1517.3s, 1485.1w, 1464.6m, 1432.3m, 1341.6m, 1280.1s, 1239.1s, 1212.8m, 1186.3w, 1136.6w, 1092.5s, 1051.7w, 1016.5w, 952.1w, 884.6s, 814.4s, 703.1s, 679.6m, 644.5m, 618.1m, 542.0w, 524.4s, 503.8m cm^{-1}.

Synthesis of $\{[Cd_3(\mu_2\text{-}L_2)_3(dca)_6]\cdot0.75H_2O\}_n$ (6). A mixture of $Cd(NO_3)_2\cdot6H_2O$ (69 mg, 0.20 mmol), L_2 (29 mg, 0.2 mmol), $NaN(CN)_2$ (36 mg, 0.4 mmol), and water (10 mL) was stirred for 5 h and filtered. The filtrate was kept in a $CaCl_2$ desiccator. After a few days, colorless crystals suitable for X-ray diffraction were obtained, yield 32% (based on Cd(II) salts). Anal. Calc. for $C_{22}H_{13}Cd_2N_{20}O_{0.5}$: C, 33.43; H,1.66; N, 35.44%. Found: C, 33.46; H,1.68; N, 35.50%. IR (KBr): ν = 3522.7w, 3476.3m, 3231.3m, 3120.3m, 3101.9m, 3041.7w, 2301.7s, 2260.1s, 2209.2s, 2144.4bs, 1622.4w, 1578.2m, 1527.9s, 1465.8w, 1436.4m, 1362.4s, 1327.0s, 1262.6m, 1238.3s, 1191.1m, 1126.1w, 1102.3m, 1052.2m, 1019.5s, 978.1m, 922.1m, 847.7m, 809.7m, 715.2w, 697.4s, 650.1m, 623.5m, 526.0s, 413.7w cm^{-1}.

Synthesis of $[Cd(\mu_2\text{-}L_2)(\mu_3\text{-}SO_4)(H_2O)]_n$ (7). A mixture of $CdSO_4\cdot8H_2O$ (77 mg, 0.1 mmol), L_2 (44 mg, 0.3 mmol), and water (10 mL) was stirred for 5 h and filtered. The filtrate was kept in a $CaCl_2$ desiccator. After a few days, colorless crystals suitable for X-ray diffraction were obtained, yield 39% (based on Cd(II) salts). Anal. Calc. for $C_7H_8CdN_4O_5S$: C, 22.56; H, 2.16; N, 15.04%. Found: C, 22.46; H, 2.20; N, 15.10%. IR (KBr): ν = 3380.5w, 3344.3w, 3275.2w, 3147.1m, 3095.6m, 3027.4w, 2941.2w, 2847.7w, 2761.8w, 2660.4w, 2459.5w, 2292.3w, 2113.2w, 1652.2m, 1618.3m, 1522.4s, 1399.6s, 1280.7m, 1170.4s, 1117.8s, 1022.9m, 885.9m, 813.4m, 694.6m, 621.3m, 460.1w cm^{-1}.

Crystal structure determination

Diffraction intensities for seven complexes were collected on a computer-controlled Bruker SMART 1000 CCD diffractometer equipped with graphite-monochromated Mo-Kα radiation with radiation wavelength 0.71073 Å using the ω-scan technique. Lorentz polarization and absorption corrections were applied. The structures were solved by direct methods and refined with full-matrix least-squares techniques using the SHELXS-97 and SHELXL-97 programs.[37] Anisotropic thermal parameters were assigned to all non-hydrogen atoms. The organic hydrogen atoms were generated geometrically; the hydrogen atoms of the water molecules were located from difference maps and refined with isotropic temperature factors. Analytical expressions of neutral-atom scattering factors were employed, and anomalous dispersion corrections were incorporated. The crystallographic data and selected bonded lengths and angles for **1**–**7** are listed in Tables 1 and 2, respectively.

CCDC reference numbers 253304–253306, 253308, 266097, 266224 and 266847.

For crystallographic data in CIF or other electronic format see DOI: 10.1039/b508332j

Results and discussion

Structures of 1–7

A view of the molecular structure of **1**, together with its numbering scheme, is depicted in Fig. 1. The structure of **1** consists of an asymmetric binuclear molecule in which two independent Cd(II) ions are bridged *via* three N1,N2-bridged triazole rings of three L_1 ligands. The Cd1 atom is six-coordinate, also bonding to one nitrate anion, one water molecule and one monodentate L_1 to complete a distorted octahedral geometry. Although the nitrate anion was bidentate at Cd2, it had a small bite angle and effectively occupied one coordination site, allowing a pseudo-octahedral description of the geometry. The distance between Cd2 and the two oxygen atoms of the bidentate nitrate anion are 2.602 and 2.585 Å, respectively, which are significantly longer than the Cd1–$O_{NO_3^-}$ (2.373 Å) distance. There are two non-coordinated nitrate anions in the

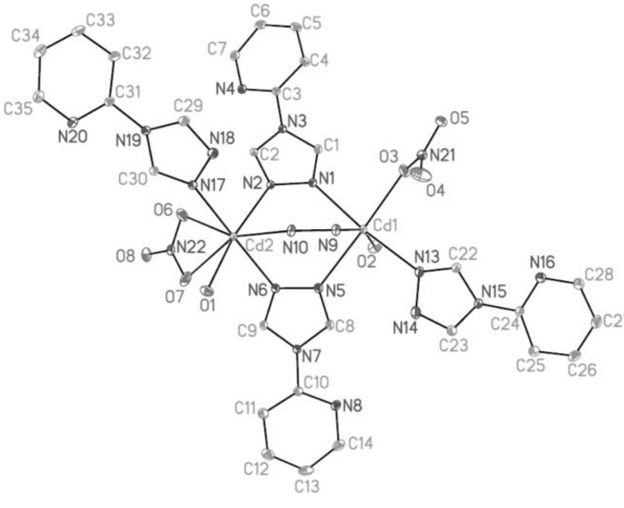

Fig. 1 An ORTEP drawing and atomic labeling system showing the structure of **1**.

Table 1 Crystal data and structure refinement information for compounds **1**–**7**

	1	**2**	**3**	**4**	**5**	**6**	**7**
Empricial formula	$C_{35}H_{33.50}Cd_2N_{24}O_{15.75}$	$C_{16}H_{12}CdN_{10}S_2$	$C_{18}H_{12}CdN_{14}$	$C_{18}H_{16}CdN_8O_2S_2$	$C_{36}H_{24}Cd_2N_{28}$	$C_{22}H_{13}Cd_2N_{20}O_{0.50}$	$C_7H_8CdN_4O_5S$
M	1267.16	520.88	536.82	552.91	1073.63	790.32	372.63
Crystal system	Triclinic	Triclinic	Orthorhombic	Triclinic	Monoclinic	Triclinic	Monoclinic
Space group	$P\bar{1}$	$P\bar{1}$	*Pbcn*	$P\bar{1}$	$P2(1)/c$	$P\bar{1}$	$P2(1)$
a/Å	11.642(6)	5.8103(9)	12.233(4)	9.9290(17)	9.7470(10)	7.7347(10)	5.4376(15)
b/Å	12.611(6)	8.3849(13)	7.277(2)	10.0981(18)	7.4296(8)	13.7682(17)	18.426(5)
c/Å	19.317(9)	10.2837(16)	22.578(7)	10.9452(19)	14.2432(15)	14.1403(18)	5.5827(16)
α/°	92.038(7)	84.804(2)		87.578(3)		111.1800(10)	
β/°	105.963(6)	81.042(2)		74.968(2)	94.1910(10)	93.100(2)	104.483(4)
γ/°	116.004(7)	87.070(2)		85.958(3)		96.835(2)	
V/Å^3	2410(2)	492.52(13)	2010.0(11)	1056.9(3)	1028.68(19)	1386.5(3)	541.6(3)
Z	2	1	4	2	1	2	2
$F(000)$	1267	258	1064	552	532	770	364
ρ/Mg m^{-3}	1.746	1.756	1.774	1.737	1.733	1.893	2.285
μ/mm^{-1}	0.976	1.346	1.128	1.265	1.102	1.591	2.230
Data/restraints/params	9803/6/731	1725/0/133	2056/0/156	3708/3/280	1809/0/151	4858/0/409	1785/1/163
GOF	1.063	1.037	1.126	1.066	1.050	1.049	1.069
$R1^a$ ($I = 2\sigma(I)$)	0.0358	0.0451	0.028	0.0358	0.0189	0.0213	0.0189
$wR2^a$ (all data)	0.0548	0.1120	0.063	0.1030	0.0554	0.0554	0.0485

[a] $R_1 = \Sigma ||F_o| - |F_c|| / |F_o|$, $wR_2 = [\Sigma w(F_o^2 - F_c^2)^2 / \Sigma w(F_o^2)^2]^{1/2}$.

Table 2 Selected bond lengths (Å) and bond angles (°) for **1–7**

1					
Cd(1)–N(13)	2.271(3)	Cd(1)–N(1)	2.327(3)	Cd(2)–O(6)	2.602(4)
Cd(1)–O(2)	2.333(3)	Cd(1)–N(9)	2.337(3)	Cd(2)–N(10)	2.449(3)
Cd(1)–O(3)	2.373(3)	Cd(1)–N(5)	2.385(3)	Cd(2)–O(7)	2.585(5)
Cd(2)–N(6)	2.348(3)	Cd(2)–O(1)	2.305(3)	Cd(2)–N(2)	2.354(3)
Cd(2)–N(17)	2.298(3)				
N(2)–Cd(2)–N(10)	85.69(11)	N(17)–Cd(2)–O(7)	109.46(12)	N(13)–Cd(1)–N(1)	172.02(12)
N(1)–Cd(1)–O(2)	91.44(12)	N(13)–Cd(1)–N(9)	96.39(12)	N(13)–Cd(1)–O(2)	83.47(13)
N(1)–Cd(1)–N(9)	90.36(11)	O(2)–Cd(1)–N(9)	161.84(13)	N(10)–Cd(2)–O(6)	159.75(12)
N(13)–Cd(1)–O(3)	93.86(12)	N(1)–Cd(1)–O(3)	79.47(11)	O(7)–Cd(2)–O(6)	47.97(11)
O(2)–Cd(1)–O(3)	84.22(14)	N(9)–Cd(1)–O(3)	113.87(13)	N(6)–Cd(2)–O(6)	105.54(11)
N(13)–Cd(1)–N(5)	91.27(13)	N(9)–Cd(1)–N(5)	81.94(12)	N(2)–Cd(2)–O(6)	77.70(11)
O(3)–Cd(1)–N(5)	162.64(12)	N(17)–Cd(2)–O(1)	90.51(12)	O(1)–Cd(2)–O(6)	113.45(11)
N(17)–Cd(2)–N(6)	175.02(11)	O(1)–Cd(2)–N(6)	86.56(12)	N(17)–Cd(2)–O(6)	79.33(11)
N(1)–Cd(1)–N(5)	93.90(12)	O(2)–Cd(1)–N(5)	79.90(13)	N(10)–Cd(2)–O(7)	152.03(12)
N(17)–Cd(2)–N(2)	91.46(11)	O(1)–Cd(2)–N(2)	168.85(11)	N(2)–Cd(2)–O(7)	113.02(12)
N(6)–Cd(2)–N(2)	90.65(11)	N(17)–Cd(2)–N(10)	89.72(11)	N(6)–Cd(2)–O(7)	73.77(12)
		N(6)–Cd(2)–N(10)	85.94(12)	O(1)–Cd(2)–O(7)	76.53(12)
2					
Cd(1)–N(10)	2.28(2)	Cd(1)–N(9)	2.27(2)	Cd(1)–S(2)	2.716(6)
Cd(1)–N(1)	2.393(13)	Cd(1)–N(5)	2.36(2)	Cd(1)–S(1)	2.753(5)
N(10)–Cd(1)–N(9)	177.5(12)	N(10)–Cd(1)–N(1)	87.5(8)	S(2)–Cd(1)–S(1)	179.6(3)
N(9)–Cd(1)–N(1)	90.0(7)	N(10)–Cd(1)–N(5)	96.6(8)	N(5)–Cd(1)–S(1)	90.9(5)
N(9)–Cd(1)–N(5)	85.9(8)	N(1)–Cd(1)–N(5)	174.8(8)	N(9)–Cd(1)–S(1)	85.9(4)
N(10)–Cd(1)–S(2)	85.6(5)	N(9)–Cd(1)–S(2)	94.5(4)	N(10)–Cd(1)–S(1)	94.1(5)
N(1)–Cd(1)–S(2)	88.1(4)	N(5)–Cd(1)–S(2)	89.1(5)	N(1)–Cd(1)–S(1)	92.0(4)
3					
Cd(1)–N(1)	2.292(2)	Cd(1)–N(7B)	2.335(3)	Cd(1)–N(5)	2.386(3)
N(5A)–Cd(1)–N(5)	92.84(15)	N(1A)–Cd(1)–N(1)	176.40(13)	N(1)–Cd(1)–N(7B)	89.90(9)
N(7B)–Cd(1)–N(7C)	93.83(16)	N(1)–Cd(1)–N(7C)	92.56(9)	N(1)–Cd(1)–N(5)	89.57(9)
N(7C)–Cd(1)–N(5)	177.81(9)	N(1)–Cd(1)–N(5A)	87.95(9)	N(7B)–Cd(1)–N(5)	86.71(11)
4					
Cd(1)–N(2)	2.270(3)	Cd(1)–N(1)	2.272(4)	Cd(1)–N(3)	2.397(3)
Cd(1)–O(1)	2.328(3)	Cd(1)–O(2)	2.366(3)	Cd(1)–N(6)	2.390(3)
N(2)–Cd(1)–N(1)	178.60(14)	O(2)–Cd(1)–N(3)	94.77(11)	N(1)–Cd(1)–N(3)	88.21(12)
N(1)–Cd(1)–O(1)	93.01(13)	N(2)–Cd(1)–O(1)	88.36(13)	O(1)–Cd(1)–N(6)	92.50(11)
N(1)–Cd(1)–O(2)	88.05(12)	N(2)–Cd(1)–O(2)	90.60(13)	N(2)–Cd(1)–N(3)	91.52(12)
N(2)–Cd(1)–N(6)	90.82(13)	O(1)–Cd(1)–O(2)	175.36(9)	O(1)–Cd(1)–N(3)	89.77(11)
O(2)–Cd(1)–N(6)	82.99(11)	N(1)–Cd(1)–N(6)	89.40(12)	N(6)–Cd(1)–N(3)	176.78(10)
5					
Cd(1)–N(5)	2.317(2)	Cd(1)–N(7B)	2.325(2)	Cd(1)–N(4)	2.335(17)
N(7C)–Cd(1)–N(4A)	88.78(7)	N(5)–Cd(1)–N(4A)	90.26(7)	N(5)–Cd(1)–N(4)	89.74(7)
N(5)–Cd(1)–N(5A)	180.00(8)	N(5)–Cd(1)–N(7B)	89.78(8)	N(7B)–Cd(1)–N(4)	88.78(7)
N(5)–Cd(1)–N(7C)	90.22(8)	N(7B)–Cd(1)–N(7C)	180.0	N(4A)–Cd(1)–N(4)	180.0
N(5A)–Cd(1)–N(4)	90.26(7)	N(7C)–Cd(1)–N(4)	91.22(7)		
6					
Cd(1)–N(17A)	2.321(2)	Cd(1)–N(1C)	2.342(2)	Cd(2)–N(15)	2.356(2)
Cd(1)–N(8)	2.372(2)	Cd(2)–N(18)	2.278(2)	Cd(2)–N(4)	2.365(2)
Cd(2)–N(5)	2.298(2)	Cd(2)–N(20F)	2.336(3)	Cd(3)–N(9F)	2.324(3)
Cd(3)–N(12)	2.300(3)	Cd(2)–N(14)	2.360(3)	Cd(3)–N(11)	2.375(3)
N(1C)–Cd(1)–N(8E)	88.27(8)	N(20F)–Cd(2)–N(4)	174.18(8)	N(17A)–Cd(1)–N(17B)	180.0(2)
N(18)–Cd(2)–N(20F)	96.06(9)	N(14)–Cd(2)–N(4)	86.68(9)	N(17B)–Cd(1)–N(1C)	87.14(8)
N(18)–Cd(2)–N(15)	93.23(9)	N(12)–Cd(3)–N(9F)	94.23(10)	N(1C)–Cd(1)–N(1D)	180.00(8)
N(20F)–Cd(2)–N(15)	87.25(9)	N(12)–Cd(3)–N(11)	93.69(11)	N(17B)–Cd(1)–N(8E)	89.22(8)
N(5)–Cd(2)–N(14)	88.71(8)	N(9F)–Cd(3)–N(11)	94.66(12)	N(18)–Cd(2)–N(5)	91.69(9)
N(15)–Cd(2)–N(14)	86.53(9)	N(12)–Cd(3)–N(11G)	86.31(11)	N(5)–Cd(2)–N(20F)	90.95(9)
N(5)–Cd(2)–N(4)	93.69(8)	N(17A)–Cd(1)–N(1C)	92.86(8)	N(5)–Cd(2)–N(15)	174.91(8)

Table 2 (*Contd.*)

N(15)–Cd(2)–N(4)	87.83(8)	N(1D)–Cd(1)–N(8E)	91.73(8)	N(18)–Cd(2)–N(14)	174.00(10)
N(12)–Cd(3)–N(12G)	180.0	N(17A)–Cd(1)–N(8E)	90.78(8)	N(20F)–Cd(2)–N(14)	89.92(10)
N(12)–Cd(3)–N(9C)	85.77(10)	N(9C)–Cd(3)–N(11)	85.34(12)	N(18)–Cd(2)–N(4)	87.32(8)
7					
Cd(1)–O(5)	2.276(3)	Cd(1)–O(1)	2.289(2)	Cd(1)–O(3B)	2.314(2)
Cd(1)–N(4A)	2.310(4)	Cd(1)–O(4C)	2.334(2)	Cd(1)–N(1)	2.338(4)
O(1)–Cd(1)–N(4A)	89.27(12)	O(5)–Cd(1)–N(4A)	87.89(12)	O(1)–Cd(1)–O(4C)	90.16(9)
O(1)–Cd(1)–O(3B)	166.44(9)	O(5)–Cd(1)–O(3B)	83.31(11)	O(3B)–Cd(1)–O(4C)	103.41(9)
O(5)–Cd(1)–O(4C)	168.15(11)	N(4A)–Cd(1)–O(3B)	92.62(15)	O(1)–Cd(1)–N(1)	93.16(12)
N(4A)–Cd(1)–O(4C)	82.11(11)	N(4A)–Cd(1)–N(1)	169.82(11)	O(3B)–Cd(1)–N(1)	87.34(15)
O(5)–Cd(1)–N(1)	102.20(12)	O(4C)–Cd(1)–N(1)	88.00(11)	O(5)–Cd(1)–O(1)	83.34(10)

Symmetry transformations used to generate equivalent atoms: for **1**: A: $-x + 1, -y, -z + 1$. For **2**: A: $x + 1, y, z$; B: $x - 1, y, z$. For **3**: A: $-x + 1, y, -z + 3/2$; B: $-x + 1/2, y - 1/2, z$; C: $x + 1/2, y - 1/2, -z + 3/2$; D: $x - 1/2, y + 1/2, -z + 3/2$. For **5**: A: $-x + 2, -y, -z + 2$; B: $-x + 2, -y + 1, -z + 2$; C: $x, y - 1, z$; D: $x, y + 1, z$. For **6**: A: $-x + 1, -y + 1, -z + 1$; B: $x - 1, y - 1, z - 1$; C: $-x, -y, -z + 1$; D: $x, y, z - 1$; E: $-x, -y, -z$; F: $x + 1, y, z$; G: $-x + 1, -y, -z + 1$; H: $x, y, z + 1$; I: $x - 1, y, z$; J: $x + 1, y + 1, z + 1$. For **7**: A: $-x + 1, y - 1/2, -z + 1$; B: $x - 1, y, z - 1$; C: $x - 1, y, z$; D: $x + 1, y, z + 1$; E: $x + 1, y, z$; F: $-x + 1, y + 1/2, -z + 1$.

structural unit of **1**. These non-coordinated nitrate anions and the lattice water molecules link the coordinated nitrate anions and coordinated water molecules of neighboring binuclear molecules to form a 2D hydrogen-bonding supramolecular structure, where the hydrogen bond distances (2.689 to 2.908 Å) fall in the normal range. The distance between the pyridine rings in the bridged L$_1$ ligands of two neighboring binuclear molecules is 3.535 Å, exhibiting significant π–π interactions. Intermolecular hydrogen bonds and π–π interactions in **1** play an important role in the stabilization of the crystal structure. In the FT-IR spectra, the strong asymmetric and symmetric stretching vibration bands are located at 1396.9 cm^{-1} (unusually sharp and strong) and 1025.4 cm^{-1}, respectively. It is difficult to distinguish the vibration spectra of the monodendate nitrate anion and chelating nitrate anion (1473.2m, 1396.9s and 1241.2m cm^{-1}).[38] Five coordination modes of the nitrate anions have been reported in previous papers,[39] while in the triazole–metal compounds, the coexistence of monodentate, bidentate and free nitrate anions has scarcely been reported.[34]

SCN$^-$ is a highly versatile ambidentate ligand with two donor atoms, which give rise to linkage isomers or polymers and form a variety of different coordination modes in coordination polymers.[10,35a,40] When the SCN$^-$ ligand is added to the reaction system of Cd(NO$_3$)$_2$ and L$_1$, complex **2** was obtained. As shown in Fig. 2, each Cd(II) ion coordinates to two triazole nitrogen atoms of two L$_1$ ligands, two nitrogen atoms of SCN$^-$ and two sulfur atoms of another two SCN$^-$. The neighboring cadmium(II) ions are bridged by double μ-1,3-SCN$^-$ ligands to form an eight-membered ring Cd(SCN)$_2$Cd unit with a Cd···Cd separation of 5.810 Å. The Cd(μ-SCN)$_2$Cd units construct an infinite polymeric chain and L$_1$ acts as a monodentate ligand coordinated *via* its one triazole nitrogen atom. Non-classic hydrogen bonds (C–H···N, 3.353 and 3.265 Å) exist between triazole rings in L$_1$ of two neighbouring 1D chains, which further assemble 1D chains to form a 2D supramolecular structure. The two strong bands at 2110.6 cm^{-1} and 2154.6 cm^{-1} in the FT-IR spectra can be assigned to μ-1,3-SCN$^-$.[10]

Compared with SCN$^-$, the longer pseudo-halide ligand dicyanamide (dca) can also form a variety of coordination modes and has been used as a modular, topological ligand to design coordination polymers with intriguing structures.[41] To our knowledge, the dca ligand has been scarcely reported in triazole–metal coordination polymers.[34] When dicyanamide sodium was added to an aqueous solution of Cd(NO$_3$)$_2$ and L$_1$, a 2D layer complex **3** was isolated. **3** crystallized in the orthorhombic crystal system, space group *Pbcn*. As shown in Fig. 3(a), the Cd(II) center coordinates to four nitrogen atoms of four dca and two triazole nitrogen atoms of two L$_1$ ligands. The four coordinated nitrogen atoms of dca and the center Cd(II) ion are coplanar. The Cd–N$_{\mathrm{dca}}$ distances are 2.335 and 2.385 Å, respectively, which are slightly longer than the Cd–N$_{\mathrm{NCS}}$ distance in **2**, while the Cd–N$_{\mathrm{L1}}$ distance is 2.292 Å, which is slightly shorter than the Cd–N$_{\mathrm{L1}}$ distance in **1**. The Cd(II) ions are linked *via trans*-1,5-μ$_2$-dca ligands to form Cd$_4$(dca)$_4$ basic structural units, which are further self-assembled into a (4,4) 2D layer structure (Fig. 3(b)). Although *cis*-1,5-μ$_2$-dca assembled metal centers in the form of (4,4) 2D sheets have been reported previously,[41] in the present work we report a very unusual 2D M(dca)$_2$ sheet constructed *via* only *trans*-1,5-μ$_2$-dca. The packing structure of **3** shows that these 2D layers are parallel without any interpenetration.

In the reaction system of L$_1$ and Cd(II) salts, the pyridine-nitrogen atom of L$_1$ cannot coordinate because of the large spatial

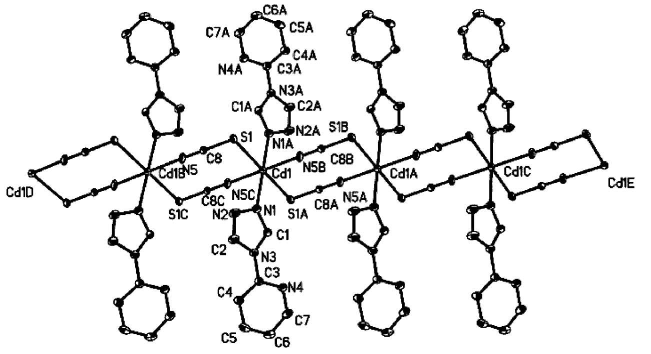

Fig. 2 An ORTEP drawing and atomic labeling system showing the 1D polymer of **2**. Symmetry codes, A: $-x + 1, -y + 2, -z + 1$; B: $x - 1, y, z$; C: $-x + 2, -y + 2, -z + 1$.

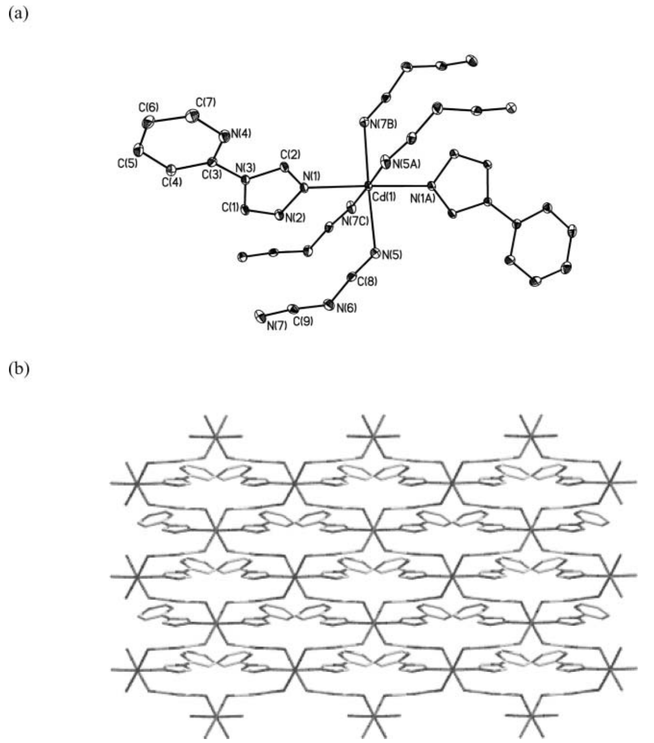

Fig. 3 An ORTEP drawing and atomic labeling system showing the coordination unit of **3** (a) and the 2D (4,4) sheet structure (b). Symmetry codes, A: $-x + 1, y, -z + 3/2$; B: $x + 1/2, y - 1/2, -z + 3/2$; C: $-x + 1/2, y - 1/2, z$.

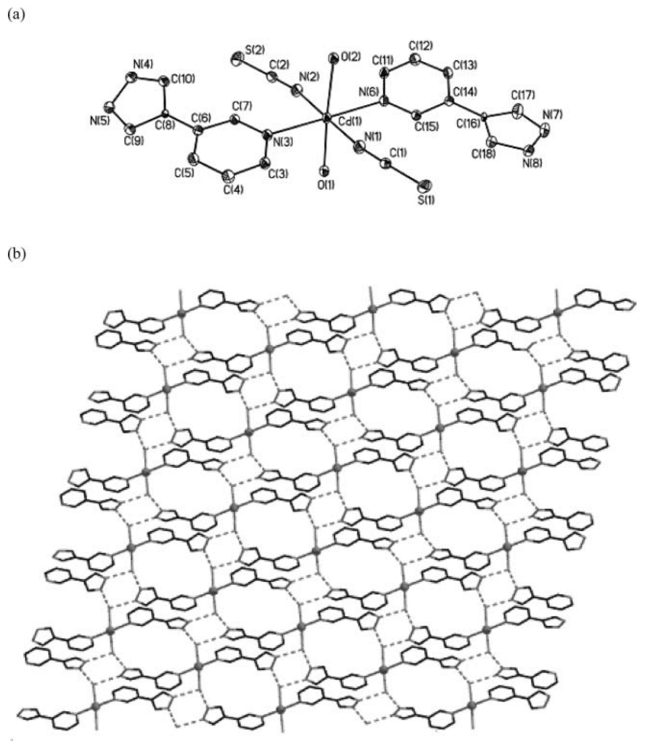

Fig. 4 An ORTEP drawing and atomic labeling system showing the structure (a) and two-dimensional supramolecular structure of **4** (b). Hydrogen bond, dotted line.

hindrance of the triazole ring. In order to investigate the effect of the 4-substituted pyridine group on the coordination motif of triazole–metal coordination polymers, the new ligand L_2 was employed. To our knowledge, complexes of L_2 have never been investigated. When SCN^- is added to an aqueous solution of $Cd(NO_3)_2$ and L_2, complex **4** is isolated. As shown in Fig. 4(a), **4** is a mononuclear complex and the cadmium(II) ion is six-coordinated by two aqua molecules, two N atoms of thiocyanate anions and two $N_{pyridine}$ atoms of L_2 ligands. The bond angles around the cadmium centre range from 88.05(12) to 94.77(11)° indicating that the cadmium ion is in a slightly distorted octahedral geometry. It is noticeable that the strong coordinated nitrogen atoms in the triazole ring of L_2 are not coordinated in **4**. As shown in Fig. 4(b), the coordinated water molecules and two nitrogen atoms of the triazole rings in neighboring L_2 ligands generate strong intermolecular hydrogen bonds (2.827 Å and 2.848 Å), which further assemble mononuclear molecules into a 2D supramolecular structure. The strong hydrogen bonds play an important role in the stabilization of the structure and what is more, prevent the triazole nitrogen atoms from coordinating to the cadmium ions to form a polymeric structure. In the FT-IR spectra, the wide and strong peak at 3635.3 cm^{-1} and strong peak at 2067.2 cm^{-1} can be assigned to hydrogen bonds and terminal thiocyanate ligand, respectively, which are in agreement with the X-ray crystal result.

When dca instead of thiocyanate anion is used in the previous reaction system, a 1D chain complex **5** is obtained. The cadmium ion is six-coordinated to two $N_{triazole}$ atoms of the ligands and four nitrogen atoms of four dicyanamide anions with an inversion symmetry. It is noted that only the nitrogen atom of the triazole group is coordinated to the cadmium(II) ions, which is different from that in **4**. The dihedral angle formed between the pyridine and triazole rings in L_2 is 39.2°, which is considerably larger than that in **4** (24.9 and 12.7°), indicating that there is a strong spatial distortion effect in **5**. The 1,5-μ_2-bridging dca ligands as double bridges link Cd(II) ions to form a 1D chain, which has similar topology to that of **2**. Although the ligands in **3** and **5** have the same terminal $N_{triazole}$, the $Cd(dca)_2$ basic unit is similar to the $Cd(NCS)_2$ unit in **2** but different from the $Cd_4(dca)_4$ basic unit in **3**, which may be due to the greater spatial torsion effect of the pyridine groups and the triazole groups. It is interesting that there are three kinds of non-classic hydrogen bonds (C(11)–H · · · N(12), 3.28 Å; C(13)–H · · · N(11), 3.48 Å; C(14)–H · · · N(20), 3.35 Å) in the packing structure (Fig. 5(b)), which help stabilize the crystal and produce a large torsion angle between the triazole and pyridine rings in L_2 to meet the forming of hydrogen bonds. The three strong peaks at 2294.1, 2225.4 and 2161.1s cm^{-1} in the FT-IR spectra can be assigned to 1,5-μ_2-bridging dca.

When we changed the ratio of Cd to L_2 from 1 : 2 to 1 : 1 in the reaction system of **5**, an unexpected 3D coordination polymer **6** was prepared. The X-ray single-crystal diffraction results reveal that there are three independent cadmium centers in **6**: Cd1 is six-coordinate, bonding to four L_2 ligands and two dca ligands; Cd2 is also six-coordinate, bonding to two L_2 ligands and four dca ligands; Cd3 is coordinated to six dca ligands. A novel 2D $Cd(dca)_2$ sheet was found as shown in Fig. 6(b). Cd3 forms a 1D $Cd(dca)_2$ chain, which is very similar to the 1D chain in **5**. Cd2, Cd1 and these 1D chains are linked *via* dca ligands to form a 2D $Cd(dca)_2$ layer. Though all dca in the 2D $Cd(dca)_2$ sheet are

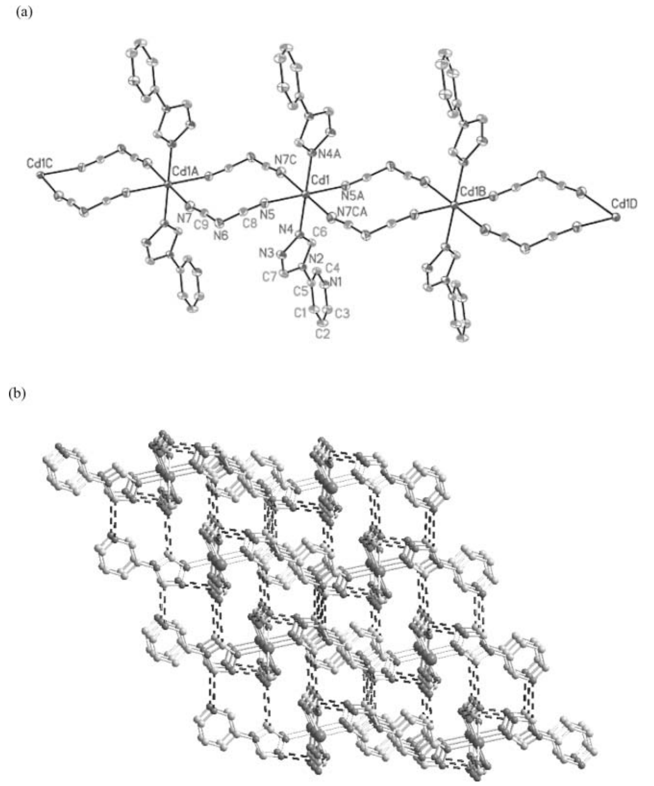

Fig. 5 An ORTEP drawing and atomic labeling system showing the 1D polymer of **5** (a) and the packing structure along the *b*-axis (b). C–H · · · N, dotted line. Symmetry codes, A: −*x* + 2, −*y*, −*z* + 2; B: −*x* + 2, −*y* + 1, −*z* + 2; C: *x*, *y* − 1, *z*.

end-to-end 1,5-μ_2-bridging through two nitrile nitrogen atoms, dca has shown extreme coordination versatility. Compared with previous results of dca complexes,[41,42] the 2D sheet in **6** exhibits a novel topology of M(dca)$_2$. A series of strong peaks (2301.7s, 2260.1s, 2209.2s, 2144.4bs cm^{-1}) in the FT-IR spectra also demonstrate the various coordination modes of dca in **6**.

Furthermore, the L$_2$ ligands link Cd1 and Cd2 between neighboring 2D layers to form a unique 3D open framework structure with different microporous channels along the *a* direction. The 2D Cd(dca)$_2$ sheets are not planar and the torsion angles between triazole and pyridine rings in L$_2$ are very large (40.6 and 58.5°) in order to meet the coordination requirements of Cd1 and Cd2. As shown in Fig. 7(a), the 3D open framework contains three kinds of 1D channel **A**, **B** and **C** with different dimensionalities and shapes. It is interesting that guest water molecules occupy channel **B** (Fig. 7(b)).

In the reaction system of Cd(dca)$_2$ and L$_2$, the lower ratio of Cd to L$_2$ (1 : 1) may induce the self-assembly of L$_2$ and Cd(II) from 1D (**5**) to 3D (**6**), which encouraged us to further investigate other Cd(II) salts and L$_2$ in the Cd to L$_2$ ratio of 1 : 1. When sulfate anions were employed in the reaction system of Cd(II) ions and L$_2$ at room temperature, a novel 3D coordination polymer **7** was isolated. As shown in Fig. 8(a), each Cd(II) ion is coordinated by three oxygen atoms from the sulfate anions and one from the coordinated water molecule, and two nitrogen atoms from a triazole ring and a pyridine ring of two L$_2$ ligands, respectively. The Cd–O distances (2.276, 2.289, 2.314, 2.334 Å) and the Cd–N distances (2.310, 2.338 Å) are similar to those of the previously reported triazole–cadmium polymers.[26a] As shown in Fig. 8(b), the structure of **7** contains a 2D layer of CdSO$_4$ along the crystallographic *b* axis. All sulfate anions adopt an unusual tridentate coordination mode to bridge three Cd(II) ions in the 2D inorganic layer. Though μ_3-SO_4^{2-} has been reported in 1D CdSO$_4$ layers,[26b] to the best of our knowledge, **7** is the first complex containing a μ_3-bridging 2D CdSO$_4$ layer. The average S–O distances (1.490 Å) of the bridged oxygen in the sulfate ions are similar to what is often referred, those of sulfate anions as bridging motifs linked to a cadmium atom, where S–O bond lengths are 1.472–1.491 Å.[11,26]

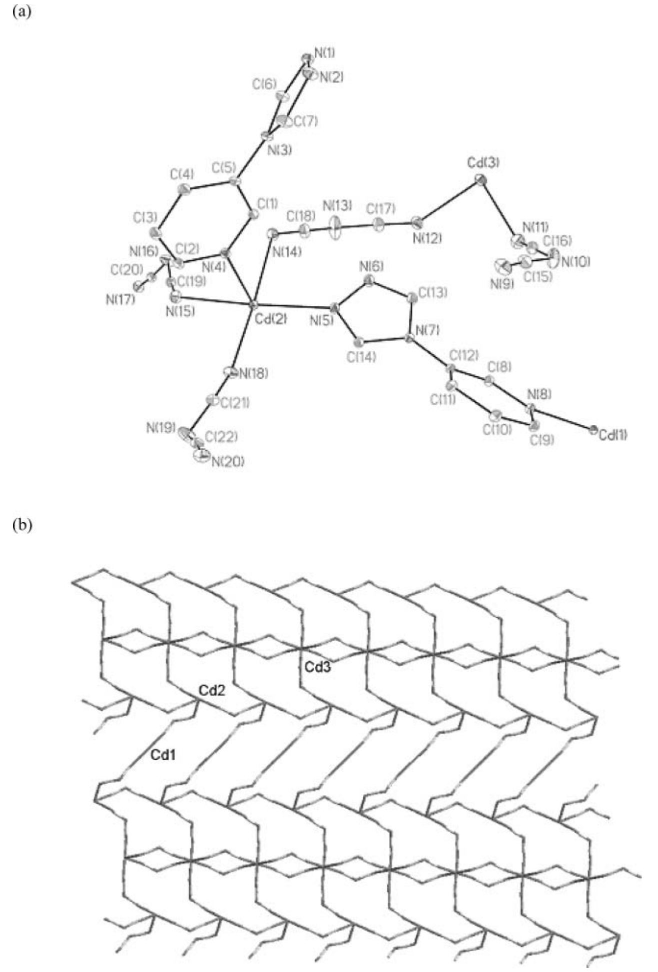

Fig. 6 Coordination fundamental unit (a) and 2D [Cd(dca)$_2$]$_n$ layer (b) of **6**.

Furthermore, L$_2$ ligands bridge two neighboring Cd(II) ions between 2D Cd–sulfate planes *via* triazole nitrogen atoms and pyridine nitrogen atoms to form a 3D open framwork structure as shown in Fig. 9. The 3D networks have 1D microporous channels, which possess approximate dimensionalities of 10.0 × 6.5 Å along the crystallographic *c* axis and 10.0 × 5.5 Å along the crystallographic *a* axis, respectively. Compared with the coordination polymers of sulfate anions with μ_2-, μ_3- and μ_4-bridging modes in previous reports,[26] **7** is prepared at room temperature rather than under hydrothermal conditions. In the FT-IR spectra, a very strong and broad peak at 1117.8 cm^{-1} and a medium peak at 621.3 cm^{-1} can be attributed to the coordinated sulfate ions.[26]

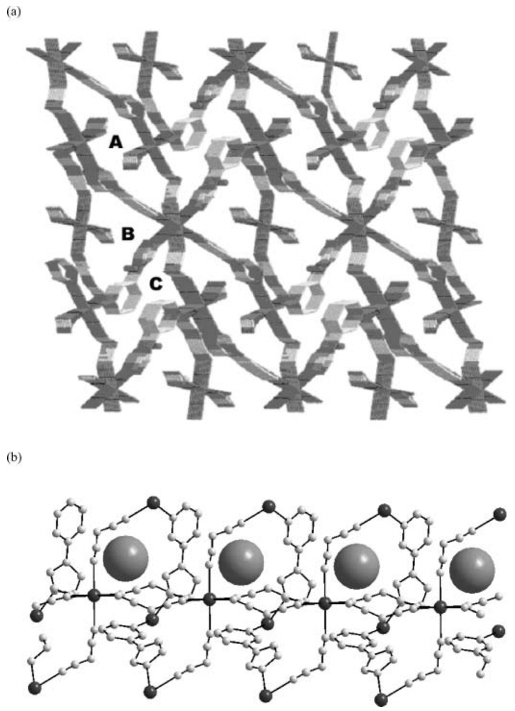

Fig. 7 The 3D open framework along the *a* direction (a) and the side view of the 1D channel **B** containing guest water molecules (as shown by the medium-gray big ball) (b) of **6**.

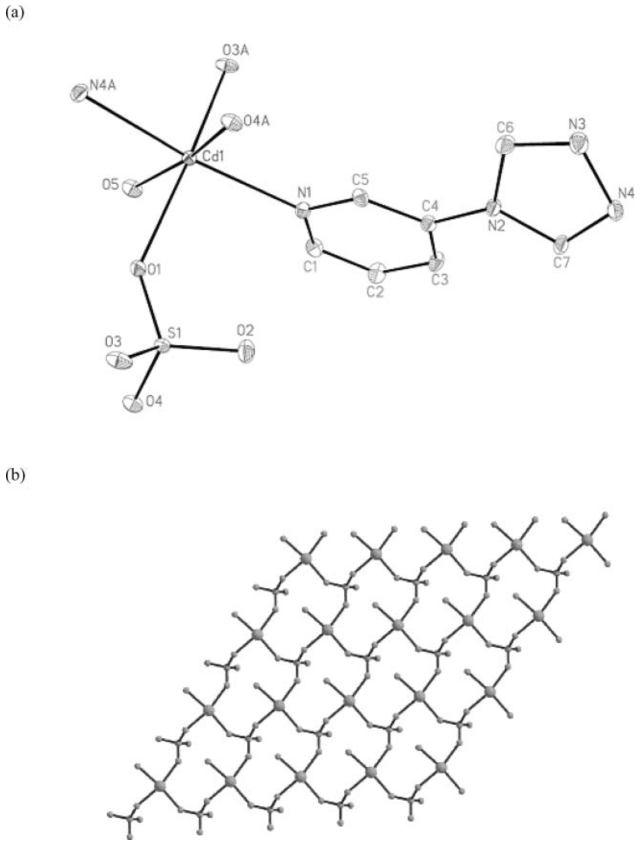

Fig. 8 Coordination fundamental unit (a) and 2D $[Cd(SO_4)(H_2O)]_n$ layer (b) of **7**. Symmetry code, A: $-x + 1, y - 1/2, -z + 1$.

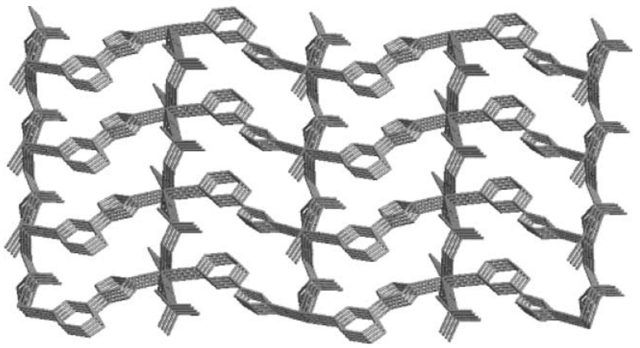

Fig. 9 The 3D framework of **7** along the *a*-axis.

Reactions and supramolecular frameworks

The generation of supramolecular frameworks rests on various parameters, such as the coordination environments of metal centers, position and type of functional groups on the ligands, the ratio between metal salts and ligands, templates, solvent system, counterions, temperature, reaction time, pH value, *etc.*[43] Complexes **1–7** are synthesized *via* a self-assembly process at room temperature and the formation and topologies of these complexes are shown in Scheme 1. From Scheme 1, it is clear that the choice of bridged anion is clearly critical in forming coordination polymers and stabilizing the structural dimensionality. When SCN^-, dca and SO_4^{2-} were added to the reaction system of $Cd(NO_3)_2$ and L_1 or L_2, they acted as bridges to link metal centers to form polymers. Compared with SCN^-, the longer dca can increase the structural dimensionality from 1D (**2**) to 2D (**3**) and from mononuclear (**4**) to 1D (**5**). The supramolecular interactions also play an important role in determining the crystal structure. In our previous report of triazole–cadmium complexes, different supramolecular assemblies induce the same CdN_4O_2 polyhedra to form 1D and 2D coordination polymers.[35a] In this work, though L_1 and L_2 act as similar terminal ligands in **3** and **5**, respectively, the pyridine nitrogen atoms in L_2 form C–H···N hydrogen bonds, which produce large torsion angles between the triazole and pyridine rings preventing dca from further linking Cd(II) centers to form

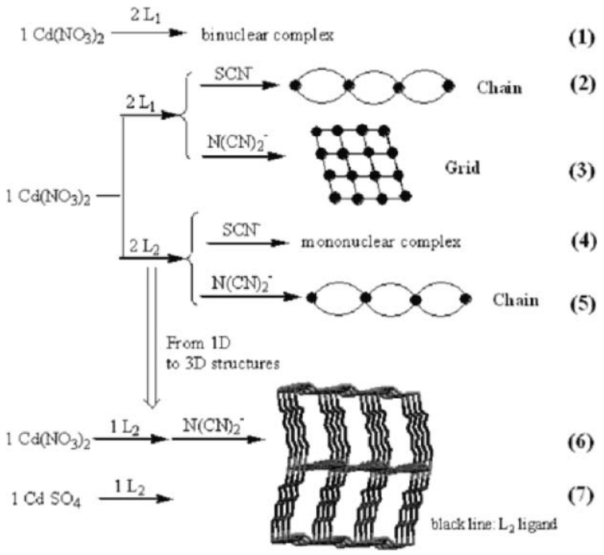

Scheme 1 Schematic drawing of reaction and topology of **1–7**.

a 2D structure. It is noted that **5** and **6** are prepared from the same reaction mixture, and the structural dimensionality increases from 1D to 3D with the reaction ratio of M to L_2. Further investigation of $CdSO_4$ with L_2 in the M to L_2 ratio of 1 : 1 also gives 3D coordination polymers. From the experimental results, we can conclude that the pyridine nitrogen in L_1 cannot coordinate to metals while L_2 is a bridging ligand able to prepare 3D microporous materials in the M to L_2 ratio of 1 : 1. Other 3D open frameworks of Cu(II) complexes (with relatively large nanoporous properties) in the M to L_2 ratio of 1 : 1 have been obtained in our lab.

Solution- and solid-state emission spectroscopy

Inorganic–organic hybrid coordination polymers have been investigated for fluorescence properties and for potential applications as luminescent materials, such as light-emitting diodes (LEDs).[44] Owing to their ability of affecting the emission wavelength and strength of organic materials, syntheses of inorganic–organic coordination polymers by the judicious choice of conjugated organic spacers and transition metal centers can be an efficient method for obtaining new types of electroluminescent materials, especially for d^{10} or d^{10}–d^{10} systems.[45] In the present work, we have explored the luminescence properties of L_1 and L_2 and organic/inorganic coordination polymers and supramolecular complexes based on the ligands in the solid-state and in water solution.

At ambient temperature, the free ligands L_1 and L_2 in H_2O solution are luminescent and show a broad emission maximum at 368 nm and 413 nm with excitation at 297 nm and 368 nm, respectively. For both ligands the chromospheres are the aromatic rings and the observed emission is due to π–π^* transitions. Compared with L_1, the maximum wavelength and the intensity of excitation and emission in L_2 are red-shifted and weaker, respectively, both of which are due to the different position of the nitrogen atom in the pyridine ring of the two ligands, which can form intermolecular hydrogen-bonding associations with solvent molecules.[46] In the solid state, both L_1 and L_2 exhibit similar strong blue emissions with λ_{max} = 434 nm with excitation at 383 nm. Compared with the fluorescence emissions of the two free ligands in solution, the excitations and emissions are red-shifted and narrow (Fig. 10), which are attributable to intermolecular interactions in the solid state, most likely π–π stacking interactions. The pyridine and triazole rings in L_1 and L_2 are linked in a similar position and may have a similar stacking manner, and hence L_1 and L_2 in the solid state are found to have very quantitatively similar behavior in the excitation and emission spectra.

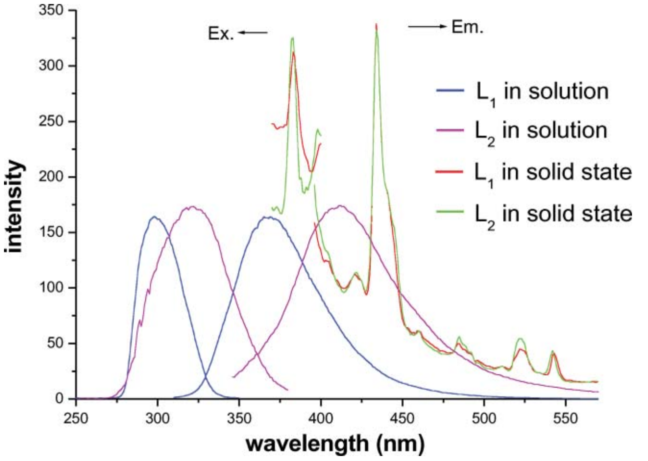

Fig. 10 Excitation and emission spectra of L_1 and L_2 in the solid state and in water solution at room temperature (1×10^{-4} mol L^{-1} for L_1 and 5×10^{-4} mol L^{-1} for L_2).

Interestingly, strong light blue fluorescence for the title complexes in the solid state is visible in daylight by irradiating with UV light. The emission spectra are shown in Fig. 11 and all the complexes are excited at 383 ± 2 nm. The main emission bands of complexes **1–5** and **7** are located in similar positions exhibiting strong blue fluorescence (λ_{max} = 434 nm) with slightly different band shapes. A clearly bathochromic shift in emission occurs in **6** (λ_{max} = 438 nm) compared with the other complexes. The different band shape in the luminescent emissions might be due to the different structural topologies of **1–7**. The emissions of **1–7** are neither metal-to-ligand charge transfer (MLCT) nor ligand-to-metal charge transfer (LMCT) in nature, and can probably be assigned to intraligand fluorescent emissions since very similar emissions are also observed for free L_1 and L_2. Compared with the free ligands, the red-shift in the intraligand fluorescence in **6** is probably due to the unique coordination of L_2 to Cd(II) increasing the ligand conformational rigidity, thereby reducing the non-radiative decay of the intraligand (π–π^*) excited state.[47] As shown in Fig. 12, all the title complexes exhibit broad blue fluorescence in H_2O solution. The fluorescence emissions of **1–7** are probably assigned to intraligand fluorescent emissions since similar behavior was also observed for free L_1 and L_2 in water solution.

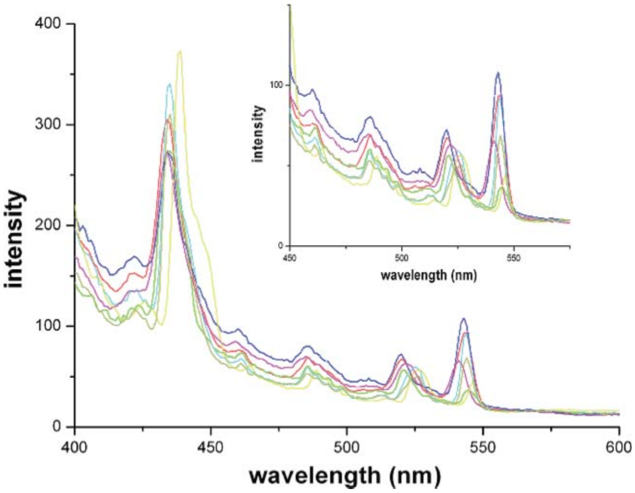

Fig. 11 Emission spectra of complexes **1–7** in the solid state at room temperature. Color lines: red, **1**; green, **2**; blue, **3**; cyan, **4**; magenta, **5**; yellow, **6**; dark yellow, **7**. All complexes are excited at 383 ± 2 nm.

TGA and PXRD of 6 and 7

The TGA of the 3D polymers **6** and **7** were determined in the range 25–800 °C in air (ESI†). The TGA of **6** between 50 °C and nearly 170 °C shows weight loss corresponding to the guest water molecules. The weight losses from 200 °C to 800 °C corresponding to the continuous decomposition of L_2 and the dca anions with concomitant formation of intermediate species. No plateau region is observed until 800 °C. The TG data

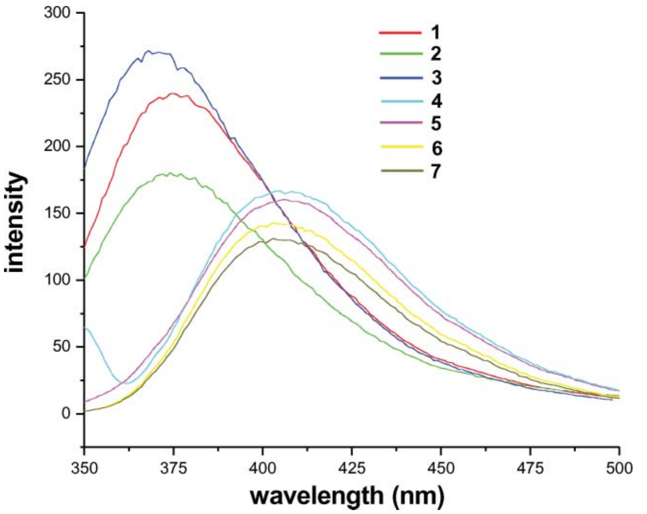

Fig. 12 Emission spectra of complexes **1–7** in water solution at room temperature (1×10^{-4} mol L^{-1} for **1–3** and 5×10^{-4} mol L^{-1} for **4–7**). Complexes **1–3** are excited at 297 ± 2 nm and complexes **4–7** are excited at 368 ± 2 nm.

for **7** show that it began to decompose at 170 °C. The weight loss in the range 170–226 °C corresponds to the release of the coordination water molecules (obsd 5.38%, calcd 4.83%). Then, the obtained $[Cd(L_2)(SO_4)]_n$ framework does not lose weight upon further heating to 280 °C. There are two weight loss stages at 280–305 °C and 390–450 °C corresponding to stepwise removal of the L_2 molecules. Finally a plateau region is observed from 605 °C to 800 °C. A white residue of $CdSO_4$ remained. The TGA results show that the 3D networks of **6** and **7** have good thermal stability in air up to 200 °C.

The crystals of **6** and **7** were heated to 200 °C under vacuum for 1 h and then characterized *via* powder X-ray diffraction (PXRD). PXRD studies were also undertaken to investigate further the characteristics of 3D coordination polymers to compare the solvate forms of the bulk materials and the single crystals. For **6**, the PXRD patterns measured for bulk solvated samples were in good agreement with the PXRD patterns simulated from the respective single-crystal X-ray data (Fig. 13). Comparison of the patterns for a solvated bulk sample and a heated sample of **6** showed that, with the exception of a few intensity differences, the patterns were in good agreement with each other. The slight shift and splitting of some peaks may be attributed to the subtle change of the relative positions of some atoms in the crystal lattice.[48] This phenomenon is commonly observed in zeolites, which indicates the distortion of micropores but does not preclude porosity and maintenance of the framework of **6**.[48,49] Thus, X-ray structural data, TGA, and powder diffraction together show that the solvents (water) in **6** can be selectively removed from the channels without destroying the channels, forming porous single crystals or powder with empty channels. For compound **7**, the PXRD patterns measured for a bulk solvated sample and a heated sample were in good agreement with the PXRD patterns simulated from the respective single-crystal X-ray data (Fig. 14), not only with respect to the positions of the peaks but also the sharpness of the lines, which confirms that the single-crystal structures are really representative of the bulk of the corresponding samples and the 3D network of **7** is stable in air up to 200 °C.

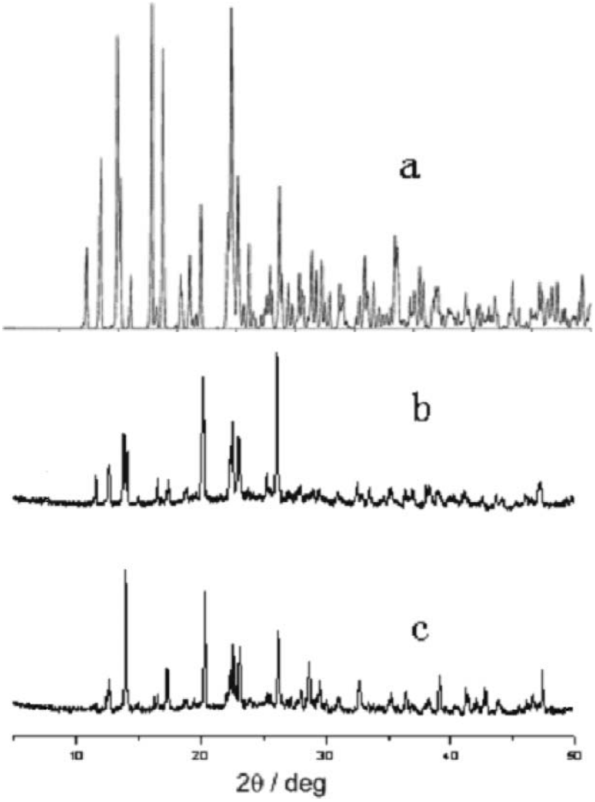

Fig. 13 X-Ray powder diffraction pattern of **6**: (a) calculated pattern from single-crystal X-ray data; (b) experimental data for crystals dried at 200 °C; (c) experimental data for solvated samples.

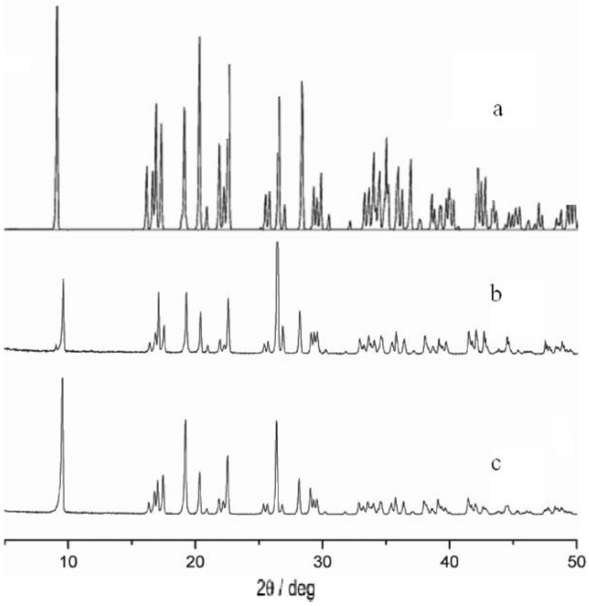

Fig. 14 X-Ray powder diffraction pattern of **7**: (a) calculated pattern from single-crystal X-ray data; (b) experimental data for crystals dried at 200 °C; (c) experimental data for solvated samples.

Conclusion

We have investigated a series of novel 4-substituted triazole–cadmium luminescent materials with a variety of zero-, one-, two-, and three-dimensional frameworks. The dca ligand is first employed in triazole–metal complexes, which gives two novel 2D M(dca)$_2$ topologies in **3** and **6**. Compared with SCN$^-$, the longer dca can also increase the structural dimensionality from 1D (**2**) to 2D (**3**) and from mononuclear (**4**) to 1D (**5**). The change in reaction ratio of Cd to L$_2$ from 1 : 2 to 1 : 1 induces 1D chain transformation into 3D framework for **5** and **6**, respectively. All the complexes exhibit strong blue fluorescence emission bands in the solid state at ambient temperature, of which excitation and emission maxima of luminescence are red-shifted to longer wavelength as compared to those in water solution. The coordinated networks of 3D microporous complexes **6** and **7** exhibit thermal stability confirmed *via* TGA and PXRD, which have potential applications in acting as molecular sieves and highly thermally stable light-emission materials. We believe that these polymers with potential properties in electrical conductivity and magnetism will be synthesized by using other transition metals with different properties than Cd(II) (such as Cu(II), Co(II), Ni(II) or Mn(II) ions). On the basis of this work, further syntheses, structures and properties studies of L$_2$ with other metals are also under way in our laboratory.

Acknowledgements

This work was supported by the National Natural Science Foundation of China (No. 90101028, 20425103) and the TRAPOYT of MOE, P. R. China.

References

1 B. F. Hoskins, R. Robson and D. Slizys, *J. Am. Chem. Soc.*, 1997, **119**, 2952.
2 B. F. Hoskins, R. Robson and D. A. Slizys, *Angew. Chem., Int. Ed. Engl.*, 1997, **36**, 2336.
3 A. H. Fu, X. Y. Huang, J. Li, T. Yuen and C. L. Lin, *Chem. Eur. J.*, 2002, **8**, 2239.
4 (*a*) B. Zhao, P. Cheng, Y. Dai, C. Cheng, D. Z. Liao, S. P. Yan, J. Z. H. Jiang and G. L. Wang, *Angew. Chem., Int. Ed.*, 2003, **42**, 934; (*b*) B. Zhao, X. Y. Chen, P. Cheng, D. Z. Liao, S. P. Yan and Z. H. Jiang, *J. Am. Chem. Soc.*, 2004, **126**, 15394; (*c*) B. Zhao, P. Cheng, X. Chen, C. Cheng, W. Shi, D. Z. Liao, S. P. Yan and Z. H. Jiang, *J. Am. Chem. Soc.*, 2004, **126**, 3012.
5 H. K. Fun, S. S. S. Raj, R. G. Xiong, J. L. Zuo, Z. Yu and X. Z. You, *J. Chem. Soc., Dalton Trans.*, 1999, 1915.
6 X. M. Chen and G. F. Liu, *Chem. Eur. J.*, 2002, **8**, 4811.
7 D. Sun, R. Cao, J. Weng, M. Hong and Y. J. Liang, *J. Chem. Soc., Dalton Trans.*, 2002, 291.
8 G. C. Guo and T. C. W. Mak, *Chem. Commun.*, 1999, 813.
9 L. Zhang, P. Cheng, L. F. Tang, L. H. Weng, Z. H. Jiang, D. Z. Liao, S. P. Yan, Z. H. Jiang and G. L. Wang, *Chem. Commun.*, 2000, 717.
10 L. Shen and Y. Z. Xu, *J. Chem. Soc., Dalton Trans.*, 2001, 3413.
11 B. Zhao, L. Yi, Y. Dai, X. Y. Chen, P. Cheng, D. Z. Liao, S. P. Yan and Z. H. Jiang, *Inorg. Chem.*, 2005, **44**, 911.
12 M. A. S. Goher, F. A. Mautner, M. A. M. A. Youssef, K. A. Hafez and A. M. A. Badr, *J. Chem. Soc., Dalton Trans.*, 2002, 3309.
13 P. M. Graham, R. D. Pike, M. Sabat, R. D. Bailey and W. T. Pennington, *Inorg. Chem.*, 2000, **39**, 5121.
14 R. Vaidhyanathan, S. Natarajan and C. N. R. Rao, *Eur. J. Inorg. Chem.*, 2003, 1675.
15 M. Kasai, M. Aoyagi and M. Fujita, *J. Am. Chem. Soc.*, 2000, **122**, 2140.
16 D. M. Shin, I. S. Lee, Y. A. Lee and Y. K. Chung, *Inorg. Chem.*, 2003, **42**, 2977.
17 M. A. Withersby, A. J. Blake, N. R. Champness, P. A. Cooke, P. Hubberstey, W. S. Li and M. Schröder, *Inorg. Chem.*, 1999, **38**, 2259.
18 D. M. Shin, I. S. Lee, Y. K. Chung and M. S. Lah, *Inorg. Chem.*, 2003, **42**, 5459.
19 C. D. Wu, C. Z. Lu, H. H. Zhuang and J. S. Huang, *J. Am. Chem. Soc.*, 2002, **124**, 3836.
20 S. S.-Y. Chui, S. M.-F. Lo, J. P. H. Charmant, A. G. Orphen and I. D. Williams, *Science*, 1999, **283**, 1148.
21 L. R. Zhang, Z. Shi, G. Y. Yang, X. M. Chen and S. H. Feng, *J. Chem. Soc., Dalton Trans.*, 2000, 275.
22 L. Yi, B. Ding, B. Zhao, P. Cheng, D. Z. Liao, S. P. Yan and Z. H. Jiang, *Inorg. Chem.*, 2004, **43**, 33.
23 M. Fujita and Y. J. Kwon, *J. Am. Chem. Soc.*, 1994, **116**, 1151.
24 X. R. Meng, Y. L. Song, H. W. Hou, Y. T. Fan, G. Li and Y. Zhu, *Inorg. Chem.*, 2003, **42**, 1306.
25 H. Zhang, X. Wang, K. Zhang and B. K. Teo, *Coord. Chem. Rev.*, 1999, **183**, 157.
26 (*a*) X. Meng, Y. Song, H. Hou, H. Han, B. Xiao, Y. Fan and Y. Zhu, *Inorg. Chem.*, 2004, **43**, 3528; (*b*) S. D. Huang, R. G. Xiong, J. Han and B. R. Weiner, *Inorg. Chim. Acta*, 1999, **294**, 95; (*c*) Y. Xu, W. Bi, X. Li, D. Sun, R. Cao and M. C. Hong, *Inorg. Chem. Commun.*, 2003, **6**, 495.
27 H. Zhang, D. E. Zelmon, G. E. Price and B. K. Teo, *Inorg. Chem.*, 2000, **39**, 1868.
28 F. Cariati, G. Ciani, L. Menabue, G. C. Pellacani, G. Rassu and A. Sironi, *Inorg. Chem.*, 1983, **22**, 1897.
29 H. Strasdeit, W. S. Pohl, W. L. Driessen and J. Reedijk, *Inorg. Chem.*, 1988, **27**, 1557.
30 P. M. Secondo, J. M. Land, R. G. Baughman and H. L. Collier, *Inorg. Chim. Acta*, 2000, **309**, 13.
31 D. W. Bruce and D. O'Hare, *Inorganic Materials*, Wiley, Chichester, UK, 1992.
32 O. Kahn, *Molecular Magnetism*, VCH, New York, 1993.
33 O. Kahn, J. Kröber and C. Jay, *Adv. Mater.*, 1992, **4**, 718.
34 J. G. Haasnoot, *Coord. Chem. Rev.*, 2000, **200–202**, 131.
35 (*a*) L. Yi, X. Yang, P. Cheng and T. B. Lu, *Cryst. Growth Des.*, 2005, **5**, 1215; (*b*) L. Yi, L.-N. Zhu, B. Ding, P. Cheng, D.-Z. Liao, S.-P. Yan and Z.-H. Jiang, *Inorg. Chem. Commun.*, 2003, **6**, 1209; (*c*) B. Ding, L. Yi, L. N. Zhu, P. Cheng and D. Z. Liao, *J. Coord. Chem.*, 2004, **57**, 9; (*d*) L. Yi, L. N. Zhu, P. Cheng, D. Z. Liao, Y. P. Zhai, S. P. Yan and Z. H. Jiang, *Transition Met. Chem.*, 2004, **29**, 200; (*e*) L. Yi, J. Y. Du, S. Liu and X. Wang, *J. Chem. Res., Synop.*, 2004, 29; (*f*) B. Ding, H. M. Wang, L. Yi, P. Cheng, L. C. Li, Y. B. Zhai, D. Z. Liao, S. P. Yan and Z. H. Jiang, *Chin. Sci. Bull.*, 2003, **48**, 2446.
36 R. H. Wiley and A. J. Hart, *J. Org. Chem.*, 1953, **18**, 1368.
37 (*a*) G. M. Sheldrick, *SHELXL-97, Program for the Solution of Crystal Structures*, University of Göttingen, Germany, 1997; (*b*) G. M. Sheldrick, *SHELXL-97, Program for the Refinement of Crystal Structures*, University of Göttingen, Germany, 1997.
38 S. Ferrer, J. G. Haasnoot, J. Reedijk, E. Muller, C. M. Biagini, M. Lanfranchi, A. M. M. Lanfredi and J. Ribas, *Inorg. Chem.*, 2000, **39**, 1859.
39 (*a*) A. B. Sarah and R. C. Neil, *Coord. Chem. Rev.*, 2003, **246**, 145; (*b*) D. B. Cordes, A. S. Bailey, P. L. C. Davies, D. H. Gregory, L. R. Hanton, K. Lee and M. D. Spicer, *Inorg. Chem.*, 2005, **44**, 2544.
40 J. G. Haasnoot, G. C. M. Keyzer and G. C. Verschoor, *Acta Crystallogr., Sect. C*, 1983, **39**, 1207.
41 (*a*) R. B. Stuart and S. M. Keith, *Coord. Chem. Rev.*, 2003, **246**, 103; (*b*) H. Sun, Z. Wang and S. Gao, *Inorg. Chem.*, 2005, **44**, 2169; (*c*) I. Dasna, S. Golhen, L. Ouahab, M. Fettouhi, O. Pena, N. Daro and J. P. Sutter, *Inorg. Chim. Acta*, 2001, **326**, 37.
42 J. L. Manson, J. A. Schlueter, U. Geiser, M. B. Stone and D. H. Reich, *Polyhedron*, 2001, **20**, 1423.
43 M. Kasai, M. Aoyagi and M. Fujita, *J. Am. Chem. Soc.*, 2000, **122**, 2140.
44 U. H. F. Bunz, *Chem. Rev.*, 2000, **100**, 1605.
45 (*a*) C. Seward, W.-L. Jia, R.-Y. Wang, G. D. Enright and S.-N. Wang, *Angew. Chem., Int. Ed.*, 2004, **43**, 2933; (*b*) V. W.-W. Yam and K. K.-W. Lo, *Chem. Soc. Rev.*, 1999, **28**, 323.
46 M. Prabhakar, P. S. Zacharias and S. K. Das, *Inorg. Chem.*, 2005, **44**, 2585.
47 C. M. Che, C. W. Wan, K. Y. Ho and Z. Y. Zhou, *New J. Chem.*, 2001, **25**, 63.
48 (*a*) T. M. Reineke, M. Eddaoudi, M. Fehr, D. Kelley and O. M. Yaghi, *J. Am. Chem. Soc.*, 1999, **121**, 1651; (*b*) K. L. Lu, Y. F. Chen, Y. H. Liu, Y. W. Cheng, R. T. Liao and Y. S. Wen, *Cryst. Growth Des.*, 2005, **5**, 403.
49 D. W. Breck, *Zeolite Molecular Sieves, Structure, Chemistry, and Use*, John Wiley & Sons, New York, 1974.